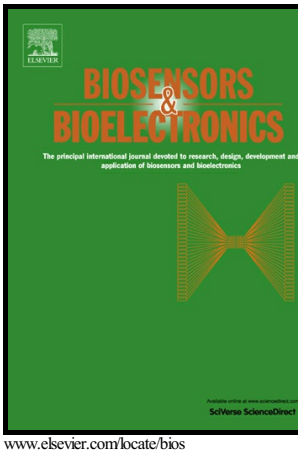

www.elsevier.com/locate/bios

Molybdenum disulphide and graphene quantum dots as electrode modifiers for laccase biosensor

Ioana Vasilescu, Sandra A.V. Eremia, Mihaela Kusko, Antonio Radoi, Eugeniu Vasile, Gabriel-Lucian Radu

PII: S0956-5663(15)30377-8
DOI: http://dx.doi.org/10.1016/j.bios.2015.08.051
Reference: BIOS7947

To appear in: *Biosensors and Bioelectronic*

Received date: 1 July 2015
Revised date: 21 August 2015
Accepted date: 22 August 2015

Cite this article as: Ioana Vasilescu, Sandra A.V. Eremia, Mihaela Kusko, Antonio Radoi, Eugeniu Vasile and Gabriel-Lucian Radu, Molybdenum disulphide and graphene quantum dots as electrode modifiers for laccas biosensor, *Biosensors and Bioelectronic* http://dx.doi.org/10.1016/j.bios.2015.08.051

Molybdenum disulphide and graphene quantum dots as electrode modifiers for laccase biosensor

Ioana Vasilescu[a], Sandra A.V. Eremia[a*], Mihaela Kusko[b], Antonio Radoi[b*], Eugeniu Vasile[c], Gabriel-Lucian Radu[a]

[a.]Centre of Bioanalysis, National Institute of Research and Development for Biological Sciences - Bucharest, 296 Splaiul Independentei, 060031, Bucharest, Romania

[b.]National Institute for Research and Development in Microtechnologies (IMT-Bucharest), 126A Erou Iancu Nicolae, 077190, Bucharest, Romania

[c] Department of Oxide Materials and Nanomaterials, Faculty of Applied Chemistry and Material Science, University Politehnica of Bucharest, No. 1-7 Gh. Polizu Street, 011061, Bucharest, Romania

[*] **Corresponding authors**:
Sandra A. V. Eremia, PhD
e-mail adress: sandraeremia@gmail.com
Tel/fax no: +40.21.220.09.00
Antonio Radoi, PhD
e-mail adress: radoiantonio@yahoo.com
Tel no: +40.21.269.07.78 / 79 (ext. 19); Fax no: +40.21.269.07.72 / 76

ABSTRACT

A nanocomposite formed from molybdenum disulfide (MoS_2) and graphene quantum dots (GQDs) was proposed as a novel and suitable support for enzyme immobilisation displaying interesting electrochemical properties. The conductivity of the carbon based screen-printed electrodes was highly improved after modification with MoS_2 nanoflakes and GQDs, the nanocomposite also providing compatible matrix for laccase immobilisation. The influence of different modification steps on the final electroanalytical performances of the modified electrode were evaluated by UV-Vis absorption and fluorescence spectroscopy, scanning electron microscopy, transmission electron microscopy, X ray diffraction, electrochemical impedance spectroscopy and cyclic voltammetry. The developed laccase biosensor has responded efficiently to caffeic acid over a concentration range of 0.38-100 µM, had a detection limit of 0.32 µM and a sensitivity of 17.92 nA μM^{-1}. The proposed analytical tool was successfully applied for the determination of total polyphenolic content from red wine samples.

Keywords: MoS_2, Graphene quantum dots, Laccase, Biosensor, Polyphenol index.

1. Introduction

Laccases are multicopper-oxidase enzymes that catalyse the one-electron oxidation processes of various phenolic compounds and aromatic amines with the concomitant reduction of oxygen (Kudanga et al., 2011). They occur widely in fungi but are also found in higher plants, prokaryotes and bacteria. Besides their use in analytical applications as biosensors and biofuel cells, laccases play an important role in food, paper, textile and pharmaceutical industry, or in cosmetics and environmental bioremediation (Shraddha et al., 2011). In recent years, laccase based biosensors are becoming relevant for areas like food analysis and environmental monitoring due to their properties such as fast response time, low-cost, low reagents consumption and the most important one, the possibility to use them in field. The ability of laccase to catalyse the one-electron oxidation of different polyphenols has been used to develop laccase based electrochemical biosensors for the determination of polyphenolic index in wines (García-Guzmán et al., 2015; Lanzellotto et al., 2014), in tea infusions (Cortina-Puig et al., 2010; Eremia et al., 2013) and tea leaves extracts (Rawal et al., 2012) as well as for the determination of environmental pollutants (Brondani et al., 2013; Nazari et al., 2015; Oliveira et al., 2013).

The tendency in the field of electrochemical biosensors is substituting the organic redox mediators with different nanomaterials such as noble metal nanoparticles (Radoi et al., 2011), carbon derived materials (Eremia et al., 2013; Karimi-Maleh et al., 2013; Karimi-Maleh et al., 2014) and transition-metal dichalcogenides and thus immobilising the enzyme at the electrode surface promoting the development of third-generation biosensors. Therefore attention has to be paid in order to obtain an efficient electron transport between the electrode and the redox active sites of the enzyme, as enzymes may exhibit reluctant electron transfer at the surface of conventional electrodes.

Molybdenum disulfide (MoS_2) is a two-dimensional (2D) layered material having a hexagonal crystalline lattice, the Mo layer being sandwiched between two S layers, the layers

being stacked by weak van der Waals interactions (Song and Kokot, 2014; Wang, 2014). Graphene on the other hand, is a revolutionary 2D material which has been intensively studied by many researchers and has potential applications in many areas. The main difference between the mentioned 2D materials is the presence of an indirect bandgap of 1.2 eV for bulk MoS_2 (or 1.8 eV for a MoS_2 monolayer) (Mak et al., 2010) in contrast to the zero-gap semiconductor graphene (Wang, 2014) that leads to an attractive electrocatalytic activity (Mao et al., 2015). The first scientific papers describing the use of MoS_2 nanomaterial in the construction of biosensors appeared in 2013; the most cited work is describing the development of a sensing platform for DNA detection (Zhu et al., 2013), while the other two articles describing biosensors based on MoS_2 nanosheets for H_2O_2 determination (T. Wang et al., 2013; G.-X Wang et al., 2013).

The tremendous interest in graphene is related to its potential electronic applications such as transistors (Schwierz, 2010), transparent electrodes (Pang et al., 2011) or photodetectors (Liu et al., 2014) despite of its zero-energy gap (Güçlü et al., 2014). The obstacle regarding graphene zero-bandgap can be eliminated by reducing the lateral size of graphene and thus opening an energy gap that is characteristic to graphene ribbons and graphene quantum dots (Güçlü et al., 2014). Graphene quantum dots (GQDs) are graphene fragments having their diameter below 20 nm that attracted considerable attention for the last years. One of the most important properties of GQDs is that they are carbon derived materials, showing low toxicity, high solubility in many solvents and the possibility of functionalization at their edges (Bacon et al., 2014). The main use of GQDs is in photovoltaic devices due to their ability to absorb a high percentage of incident light (Mihalache et al., 2015), followed by fuel cells, bio-imaging and biosensing (Bacon et al., 2014; Shen et al., 2012). Literature data revealed few papers regarding GQDs-based electrochemical biosensors. Zhao et al. have designed an electrochemical biosensor based on the interaction between GQDs and single-stranded DNA (Zhao et al., 2011), Muthurasu and Ganesh have also developed an enzymatic biosensor by anchoring horseradish

peroxidase on GQDs for the detection of H_2O_2 (Muthurasu and Ganesh, 2014), Razmi and Mohammad-Rezaei have immobilised glucose oxidase on GQDs and have obtained a performant platform for sensitive detection of glucose (Razmi and Mohammad-Rezae, 2013).

The present work wants to bring together for the first time in the field of biosensors MoS_2 and GQDs as electrode modifiers for constructing a sensitive and reusable laccase based biosensor. The conductivity of the carbon based screen-printed electrodes was highly improved when both MoS_2 nanoflakes and GQDs were added providing thus the host matrix for enzyme immobilisation. The biosensor construction was firstly realised by drop casting the carbon screen-printed electrodes (CSPEs) with successive additions of MoS_2 and GQDs dispersions, and finally *Trametes versicolor* laccase (TvL) was immobilised. It was observed that the used 2D materials enabled a better adsorption of the enzyme due to their high surface-to-volume ratio and thus the developed CSPE modified with MoS_2, GQDs and TvL based biosensor (CSPE-MoS_2-GQDs-TvL) was successfully applied for the determination of polyphenol index in red wines.

2. Experimental section

2.1. Reagents and solutions

Laccase (benzenediol: oxygen oxidoreductase EC 1.10.3.2, activity provided on the bottle $\geq$ 10 U mg^{-1}) from *Trametes versicolor* was purchased from Sigma-Aldrich (Germany) and stored at – 18 °C. The exact laccase activity was determined according to the data from the Supplementary Material. Caffeic acid, chlorogenic acid, (-) epicatechin, ABTS, potassium ferricyanide, Folin-Ciocalteu reagent, D-(+)-glucosamine hydrochloride, sodium carbonate and potassium chloride were also purchased from Sigma-Aldrich (Germany). Polyphenols stock solutions were prepared in 0.1 M acetate buffer containing 10% ethanol (*v/v*), pH 5.00 and more diluted standard solutions were prepared by suitable dilution in 0.1 M acetate buffer pH 5.00. All the reagents were of analytical grade. Poly(ethyleneimine) solution 50% (*w/v*) in H_2O was

from Fluka and molybdenum disulfide (MoS_2) was supplied, as nanoscale crystals dispersed in ethanol solution, by Graphene Supermarket.

The supporting electrolyte consisted of 0.1 M acetate buffer pH 5.00 in 0.1 M KCl. Acetate buffer solutions (0.1 M) at various pH values (ranging between 3.76–6.00 as acetate pK_a is 4.75) were used as supporting electrolytes during the biosensor optimization studies. High purity deionized water obtained from a Milli-Q system (Millipore, France) has been used to prepare all the aqueous solutions.

Some of the tested red wine samples were kindly supplied by the Institute of Research and Development for Viticulture and Oenology Valea Calugareasca (ICDVV), Romania while others were purchased from a local hypermarket in Bucharest (Romania). The wine samples pretreatment consisted of 200 times dilution in acetate buffer before biosensor analysis and 100 times in water for Folin-Ciocalteu assessment.

2.2. Instrumentation and electrodes

Spectrophotometric measurements were performed on a Thermo Evolution 260 Bio (Thermo Fisher Scientific Inc., Rockford, IL, USA). The micrographs were obtained using a Nova NanoSEM 630 (FEI Company, USA) Scanning Electron Microscope (SEM). Transmission electron microscopy (TEM) images were obtained on a Tecnai™ G2F30 S-TWIN transmission electron microscope operated at 300 kV. Diffraction patterns were collected using the 9 kW rotating anode Rigaku SmartLab thin film triple-axis diffraction system operated at U = 45 kV, I =200 mA with a CuKα radiation (λ = 1.541867 Å), in parallel beam mode. Fluorescence emission spectra were recorded at room temperature using the FLS920 spectrometer equipped with a 450 W Xenon lamp as excitation source. The absolute fluorescence quantum yield (QY) of the GQDs solution was determined using the integrating sphere setup. Zeta potential of the MoS_2 and GQDs dispersions was measured using the Delsa™Nano analyser from Beckman Coulter, USA.

The cyclic voltammetry, electrochemical impedance spectroscopy and chronoamperometry measurements were carried out using a potentiostat AutoLab PGSTAT 302N (Utrecht, Netherlands) that was equipped with GPES (4.9) Eco Chemie (Utrecht, Netherlands) software. The electrochemical cell consisted of carbon screen-printed electrodes (DRP-C150, DropSens, Spain) the working electrode having 4 mm in diameter, the counter electrode is made of Pt, while the pseudo-reference electrode and the electric contacts are made of Ag, all printed onto a ceramic support (3.4 cm × 1.0 cm). The CSPEs were connected to the potentiostat using the specific connector (DRP-DSC) from DropSens.

2.3. Synthesis of graphene quantum dots (GQDs)

Graphene quantum dots (GQDs) were synthesized by a microwave assisted single step hydrothermal route (Mihalache et al., 2014; Mihalache et al., 2015). In a typical procedure, 2.0 g of D-(+)-glucosamine hydrochloride, 3.0 g of poly(ethyleneimine) solution and 2.5 mL of distilled water were thoroughly mixed, allowed to react during 4 hours, at room temperature (24 °C). A volume of 5 mL was introduced in the reaction vessel and during 60 seconds, 700 W were applied; the reaction mixture was allowed to cool down at room temperature for 1 hour. The reaction mixture was further centrifuged at 20.000 rpm, during 1 hour, at 10 °C, using a Beckman Coulter Avanti J-30I centrifuge. The supernatant was collected and used for further experiments or stored at 4 °C. A microwave acid digestion vessel (4781 type) provided by Parr Instrument Company and a commercial microwave oven were used during synthesis.

2.4. Preparation of CSPE-MoS_2-GQDs-TvL biosensor

Carbon screen-printed electrodes from DropSens were used as biosensor substrate due to their good conductivity, reproducibility and low-cost. Firstly, 8 µL of MoS_2 nanoflakes suspension (18 mg L^{-1}) were casted on the surface of the CSPE and allowed to dry, followed by drop-casting of 6 µL of GQDs water based suspension (1:10 *v:v* dilution from the collected

supernatant). Finally, TvL immobilisation was performed by casting 5 µL from a 58.23 U mL^{-1} laccase solution onto the modified working electrode and allowed to dry in a dehumidified room at 24 °C. The resulting CSPE-MoS_2-GQDs-TvL biosensor was stored at 4 °C. Fig. 1 describes the construction approach and the working principle of the CSPE-MoS_2-GQDs-TvL biosensor, the nanocomposite formed by MoS_2 and GQDs providing an appropriate environment for laccase immobilisation at the surface of the electrode, immobilisation that occurred through electrostatic interaction between the negatively charged laccase and the positively charged GQDs. Caffeic acid is oxidised to the corresponding quinone in the presence of laccase, under acidic conditions and in the presence of molecular oxygen, the quinone being further reduced (electrochemically) at the biosensor surface. The resulting current obtained by quinone reduction is proportional to the caffeic acid concentration.

Fig. 1

2.5. Electrochemical measurements

All cyclic voltammetry (CV) and chronoamperometry (CA) measurements were performed at room temperature (24 °C ± 0.5), in drop mode, the supporting electrolyte consisting of 0.1 M acetate buffer pH 5.00 in 0.1 M KCl, and polyphenols or red wine samples were added in the electrochemical cell using a micropipette. The CV experiments were recorded by cycling the potential between +0.65 and -0.30 V at a scan rate of 50 mV s^{-1}. The CA measurements were realized at 50 mV *vs.* Ag pseudo-reference electrode, the calibration curves being performed by washing the electrode between the additions of different substrate concentrations.

To better understand the electrochemical interfacial behaviour of the electrode, in the presence and in the absence of the modifiers, *i.e.* MoS_2, GQDs and laccase, electrochemical impedance spectroscopy (EIS) studies were also performed, at frequencies ranging between 300

kHz and 0.01 Hz, with a voltage perturbation of 10 mV rms, and +130 mV applied dc bias as formal redox potential. The supporting electrolyte during EIS investigations was 0.1 M KCl solution containing 2 mM $[Fe(CN)_6]^{3-/4-}$.

3. Results and discussion

3.1. UV-Vis, fluorescence, SEM, HR-TEM and XRD characterization

Although absorption was recorded between 200 and 1100 nm, strong optical absorption appeared only in the UV region with a tail reaching the visible range. Fig. 2 (inset) shows the GQDs absorption spectrum, the main peak at 267 nm being assigned to π-π* transitions of C-O and aromatic C=C bonds present in the sp^2 hybridization region. Typically, graphene quantum dots display broad bandwidths and excitation dependent photoluminescence emissions as their main spectroscopic features, photoluminescence emission being the result of electron-hole pair recombination. Fig. 2 shows a broad bandwidth covering wavelengths mainly from visible domain (350 nm up to 650 nm). Photoluminescence emission had a constant bathochromic shift with a pronounced decrease in intensity as excitation was extended to longer wavelengths. GQDs displayed a quantum yield of 11%, measured at 340 nm excitation.

Fig. 2

The alteration of the bare CSPE surface morphology (Fig. S1.A) was achieved using MoS_2, GQDs and TvL. Scanning electron microscopy (SEM) indicated that MoS_2 was uniformly distributed (Fig. S1.B) on the surface of the electrode, while the presence of graphene quantum dots was indicated by the appearance of fuzziness and darker areas (Fig. S1.C). Laccase layer was evidenced in Fig. S1.D as a transparent membrane covering the modified electrode. Graphene quantum dots HR-TEM (Fig. S2) analysis provided the lattice parameter of 3.3 Å corresponding to the [002] facet, in agreement with the interlay distance of graphene sheets,

demonstrating the graphitic nature of the crystalline dots. Also the lattice spacing of 2.4 Å was consistent with the (1120) lattice fringes of graphene. GQDs diameters ranged between 2.8 and 4.3 nm, having an average diameter of 3.4 nm. As for the nanocomposite (Fig. S3), beside graphene characteristic lattice parameters, an interlayer distance of 6.4 Å was evidenced, being assigned to (002) orientation in MoS_2. The XRD analysis (Supplementary Material, Fig. S4) indicated for MoS_2 nanoflakes an increased interlayer distance ($\Delta c/co = + 2.82\%$) and a decrease in crystallinity, based on lower peak intensity at (002) orientation.

3.2. Electrochemical behaviour of CSPE-MoS_2-GQDs-TvL biosensor

Zeta potential measurements have shown that MoS_2 nanoflakes were negatively charged with a zeta potential of -30.4 mV, while GQDs were positively charged with a zeta potential of +4.6 mV. Therefore, laccase that is negatively charged with an isoelectric point around 3.5 (Wu et al., 2014) can be immobilised onto the GQDs surface by electrostatic interaction.

The recorded EIS spectra (Fig. S5) were analysed by means of three equivalent electrical circuits (Fig. S6, Supplementary Material). The characteristic semicircle (Fig.S5.A) that appeared in the high frequency range was ascribed to the charge-transfer resistance (R_{ct1}) and the double layer capacity (CPE_1) occurring at the interface between the electrode and the electrolyte. The R_{ct1} values were inversely proportional to the rate of electron transfer and it can be observed that while a 1.5 increase was observed when the MoS_2 sheets were casted on the bare screen printed electrode (SPE), a significant dropping (approximately 30 times less) was achieved when GQDs were used to modify the bare electrode (Table S1). The first behaviour indicates that there are electrostatic repulsive interactions between negatively charged MoS_2 sheets and $[Fe(CN)_6]^{3-/4-}$ anions. On the contrary, albeit the previous reported impedance analyses of the electrode interface modified with GQDs obtained via graphene oxide revealed their insulating nature (Mazloum-Ardakani et al., 2015), our results confirmed that the network of GQDs obtained by microwave assisted hydrothermal route supplies excellent electronic conductivity. A

further decrease was achieved when both MoS_2 and GQDs were dropped on the SPE (Fig. S5.A, inset), the R_{ct1} change being more than two orders of magnitude, illustrating the synergistic interaction between GQDs and MoS_2 sheets.

Due to the electrode porosity, surface disorder, and adsorption processes (Jorcin et al., 2006), the capacitor element is replaced by a constant phase element (CPE_1) to represent the non-ideal capacitor behaviour of the system. For GQDs modified SPE, the basic circuit was modified introducing a second parallel C/T element, related to an additional capacitance of the nanostructures–Fig. S6.B. The tangent hyperbolic element (T element) describes the impedance of finite-length diffusion processes with a reflective boundary involving thin films with electroactive substances (Soon and Loh, 2007). It completes the classic Warburg diffusion behaviour modelling the diffusion process inside the porous nanocomposite film.

The presence of the laccase layer requested the insertion of a new charge - transfer resistance (R_{ct2}) in parallel with a second constant phase element (CPE_2) in the fitting circuit in order to compensate the charge transfer involved in the polarization process–Fig. S6.C.

In order to get a better view about the nature of the mechanism involved at the electrode, Bode impedance and Bode phase angle plots were investigated. Figures S5.B and C show the frequency dependence of the impedance module and the phase angle, respectively.

Fig. S5.B showed a decrease in the impedance in the middle range frequencies, which is an indication of an improved conductivity of the modified electrodes. Furthermore, Bode phase angle diagrams exhibited a more pronounced variation: while the bare CSPE presents two time constants, with a phase angle maximum of 32° at high frequency of around 1000 Hz, and one at 0.01 Hz, when it was modified the maximum shifted to lower frequencies (Fig. S5.C).

The electrochemical characterisation of the electrode, in its various states such as CSPE (a), CSPE-MoS_2 (b), CSPE-GQDs (c) and CSPE-MoS_2-GQDs (d) was accomplished by cyclic voltammetry studies using $[Fe(CN)_6]^{3-/4-}$ (1 mM) in 0.1 M KCl solution at a scan rate of 50 mV s^{-1} (Fig. 3). The presence of a couple of redox peaks with a peak-to-peak separation (ΔE_p) of 100

mV was observed at the surface of CSPE. After modification with MoS_2 nanoflakes the ΔE_p become 120 mV and the redox peak currents intensities slightly decreased due to the repulsion existing between the negatively charged MoS_2 and negatively charged redox probe, respectively. When CSPE was modified with GQDs the ΔE_p decreased to 66 mV and the redox peak current intensities also increased that is clearly related to the good conductivity of GQDs. Finally, at the CSPE-MoS_2-GQDs surface a ΔE_p of 71 mV was obtained and the redox peak currents were 2.2 higher than the redox peak currents obtained for CSPE. This behaviour may be attributed to the good electrocatalytic activity, large surface area and high conductivity of the MoS_2 nanoflakes and GQDs nanoassembly.

Fig. 3

The interesting results obtained for MoS_2-GQDs modified electrode could be ascribed to a large increase in the surface area, resulting in an increase in real electro-active area (roughness factor) and high conductivity of the modified electrode (Table S2, Supplementary Material). The real electro-active area, A_{real} was calculated according to the following equation:

$$A_{real} = \frac{A_{R-S}}{A_G} \quad (1)$$

where A_{R-S} is the area Randles-Sevčik and it was calculated from cyclic voltammetry experiments in 1 mM $[Fe(CN)]^{3-/4-}$ solution containing 0.1 M KCl, according to Randles-Sevčik equation (Bard and Faulkner, 2001) and A_G is the geometric area of the DropSens carbon working electrode, namely 12.56 mm^2. The high real electro-active area obtained in the case of CSPE-MoS_2-GQDs modified electrode makes it a good electrochemical support for TvL immobilisation.

$$k^0 = 2.18 \left[\frac{D\alpha nvF}{RT}\right]^{1/2} \exp\left[-\left(\frac{\alpha^2 nF}{RT}\right)\ (Ep^{ox} - Ep^{red})\right] \quad (2)$$

Table S2 also reports the electron transfer rate constants (k^0) values for 1 mM $[Fe(CN)]^{3-/4-}$ calculated from cyclic voltammograms applying Kochi's method (Klingler and Kochi, 1981), see Eq. (2) considering *D* the diffusion coefficient of $[Fe(CN)_6]^{3-/4-}$ (7.6×10^{-6} cm^2 s^{-1}), α the electron transfer coefficient (0.5 for reversible reaction), *R* is the universal gas constant, *T* is the absolute temperature (K), n is the number of transferred electrons (1) and *F* is the Faraday constant. It is obvious that the electrochemical performances were improved with the modification of the electrode surface, the highest k^0 values being obtained for CSPE-MoS_2-GQDs.

Furthermore the voltammetric response of 2.5 mM caffeic acid was measured at the differently modified electrodes having immobilised laccase (300 mIU/electrode) in 0.1 M acetate buffer solution pH 5.00 at a scan rate of 50 mV s^{-1} (Fig. 4). At the CSPE-TvL modified electrode a pair of quasi-reversible peaks was observed, the reduction peak being located at approximately 0 V with an I_{pc} of 24.88 µA. When CSPE was modified with MoS_2 nanoflakes and TvL, the reduction peak had an I_{pc} of 27.98 µA and it was present at the same potential as in the case of CSPE-TvL. When the electrode was modified with GQDs and TvL, the reduction peak position has shifted to more positive values (0.11 V) and has considerably increased in current intensity, I_{pc} being 73.3 µA. And finally, when the developed CSPE-MoS_2-GQDs-TvL biosensor was tested, the reduction peak had an I_{pc} of 87.59 µA, 3.5 times higher than the current intensity of CSPE-TvL electrode and also kept its position at 0.11 V as in the case of CSPE-GQDs-TvL. The obtained results emphasise once more that the optimum base for laccase based biosensor is the CSPE-MoS_2-GQDs configuration, as confirmed by EIS investigations.

Fig. 4

The effect of the scan rate on the electrochemical response of the CSPE-MoS_2-GQDs-TvL biosensor was also studied in the presence of 2.5 mM caffeic acid (Fig. S7.A). E_{pa} shifted to more positive values and E_{pc} shifted to more negative values with the increase in the scan rate. The anodic and cathodic potentials were independent of the logarithm of the scan rate (log v) (Fig. S7.B) while anodic and cathodic peak current intensities increased linearly with the square root of the scan rate from 10 to 300 mV s^{-1} (Fig. S7.C). The latter property indicated that the process occurring at the modified electrode is a diffusion controlled process (Bard and Faulkner, 2001). However, the process is slightly influenced by the weak adsorption of caffeic acid, the effect being seen in the height of the anodic current intensity that is smaller when compared to the cathodic current intensity (Bard and Faulkner, 2001).

3.3. Optimisation of the CSPE-MoS_2-GQDs-TvL biosensor experimental parameters

The developed biosensor was optimised in terms of pH of the used buffer and applied potential. Different buffer solutions having pH values ranging between 3.76–6.00 were used and the cyclic voltammograms were registered at a scan rate of 50 mV s^{-1} (Fig. S8) using 2.5 mM caffeic acid. The cathodic peak potentials have shifted to negative values when buffer solutions pH increases from 3.76 to 6.00. The obtained slope was -65.7 mV/pH unit confirming the proton dependence of the substrate (Fig. S8 inset). The highest current intensity value was achieved at pH 5.00. The highest sensitivity of the biosensor in 0.1 M acetate buffer pH 5.00 containing 5 µM caffeic acid was obtained for an applied potential value of 50 mV *vs.* Ag pseudo-reference electrode, the enzyme loading being previously optimised (300 mIU) (Eremia et al., 2013).

3.4. Polyphenols determination

The electrochemical response of the optimised CSPE-MoS_2-GQDs-TvL biosensor toward caffeic acid was investigated using chronoamperometry at 50 mV *vs.* Ag pseudo-reference electrode, the investigated concentrations ranging between 0.38-100 µM in 0.1 M acetate buffer

pH 5.00 (Fig. S9.A). As it can be observed from Fig. S9.B, caffeic acid had two linearity domains. Chlorogenic acid and (-) epicatechin were also studied using the developed biosensor as they are commonly found in red wines together with caffeic acid.

Table 1

The analytical parameters of the developed biosensor in the determination of polyphenolic compounds, namely the linear response ranges, sensitivity, correlation coefficients, limits of detection and calculated K_m^{app} are shown in Table 1. The proposed biosensor showed linear response in the ranges of 0.38-10.00 µM and 10.00-100.00 µM for caffeic acid, 0.38-8.26 µM and 8.26-100.00 µM for chlorogenic acid and 2.86-100.00 µM for (-) epicatechin. The lowest limit of detection was obtained for chlorogenic acid while the highest for (-) epicatechin. By comparing the calculated K_m^{app} for the different substrates it was observed that the best affinity was obtained for chlorogenic acid. The analytical parameters of the proposed biosensor with respect to caffeic acid were compared to those found in literature (Table S3, Supplementary Material) and one can notice that the proposed biosensor worked at positive applied potentials, had a wide linearity domain and a very good limit of detection.

The reproducibility of the developed biosensor was checked and it was observed that for seven consecutive measurements of 30 µM caffeic acid solution the relative standard deviation was ± 10.06%. In the same time, when five different electrodes were tested in the same conditions the RSD for electrode-to-electrode reproducibility was 15.36%. The stability of the biosensor was also evaluated and the enzyme retained its activity over a period of 4 weeks, an 85.00% of the initial current intensity was obtained. These results indicated that the developed and optimised CSPE-MoS_2-GQDs-TvL biosensor is reproducible and stable for the analysis of caffeic acid.

3.5. Application to red wine samples

Table 2

The possibility of applying the developed and optimised CSPE-MoS_2-GQDs-TvL biosensor for measurements in real samples was investigated by determining total polyphenolic content from red wine samples. Before starting the polyphenol analysis ethanol (1:200, *v:v* in buffer), the main wine matrix was tested as interference but neither inhibition nor activation of laccase occurred. The results obtained using the biosensor were expressed as caffeic acid equivalents and compared with the results obtained using Folin-Ciocalteu method as reference method. As it can be seen in Table 2 the values obtained for total polyphenolic content by the two methods are in good agreement excepting the Pinot Noir and Feteasca Neagra from Beciul Domnesc for which smaller values were obtained when using the proposed biosensor. However when performing Anova test, the p-value corresponding to the F-statistic of one-way Anova was 0.38 that is higher than 0.05 suggesting that the values obtained by the two different methods for the two red wine samples were not significantly different and therefore the developed biosensor is reliable for testing red wine samples.

4. Conclusions

A laccase based biosensor using the interesting electrochemical and catalytic properties of MoS_2 nanoflakes and GQDs has been developed and characterised. Laccase was successfully immobilised by electrostatic interactions at the surface of the CSPE-MoS_2-GQDs modified electrode that is a challenging feature for enzyme based biosensors. The developed and optimised CSPE-MoS_2-GQDs-TvL biosensor exhibited wide linear ranges, 0.38-10 µM (low concentration range) and 10-100 µM (high concentration range) with a LoD of 0.32 µM and a sensitivity of 17.92 nA μM^{-1} for caffeic acid, 0.38-8.26 µM (low concentration range) and 8.26-

100.00 µM (high concentration range) with a LoD of 0.19 µM and a sensitivity of 11.25 nA μM^{-1} for chlorogenic acid and 2.86-100.00 µM with a LoD of 2.04 µM and a sensitivity of 16.42 nA μM^{-1} for (-) epicatechin. Moreover, the developed biosensor proved good stability and reproducibility in the determination of the polyphenolic compounds. Based on these observations, the combination of MoS_2 and GQDs may represent the physical foundation for the successful development of novel biosensors.

Acknowledgements

This work was financially supported by a grant of the Romanian National Authority for Scientific Research, CNDI–UEFISCDI, project number PN-II-PT-PCCA-2011-3.1-1809 and COST Action FA1403.

References

Bacon, M., Bradley, S.J., Nann, T., 2014. Part. Part. Syst. Charact. 31, 415-428.

Bard, A. J., Faulkner, L. R., 2001. Electrochemical Methods: Fundamentals and Applications. John Wiley and Sons, New York.

Brondani, D., de Souza, B., S. Souza, B., Neves, A., Vieira, C.I., 2013. Biosens. Bioelectron. 42, 242-247.

Cortina-Puig, M., Muñoz-Berbel, X., Calas-Blanchard, C., Marty, J.-L., 2010. Microchim. Acta 171, 187-193.

Eremia, S.A.V., Vasilescu, I., Radoi, A., Litescu, S.-C., Radu, G.-L., 2013. Talanta 110, 164-170.

García-Guzmán, J.J., Hernández-Artiga, M.P., Palacios-Ponce De León, L., Bellido-Milla, D., 2015. Food Chem. 182, 47-54.

Güçlü, A. D., Potasz, P., Korkusinski, M., Hawrylak, P., 2014. Berlin Heidelberg: Springer Berlin Heidelberg.

Jorcin, J.-B., Orazem, M.E., Pébère, N., Tribollet, B., 2006. Electrochim. Acta 51, 1473-1479.

Karimi-Maleh, H., Biparva, P., Hatami, M., 2013. Biosens. Bioelectron. 48, 270–275.

Karimi-Maleh, H., Tahernejad-Javazmi, F., Ensafi, A.A., Moradi, R., Mallakpour, S., Beitollahi, H., 2014. Biosens. Bioelectron. 60, 1-7.

Klingler, R.J., Kochi, J.K., 1981. J. Phys. Chem. 85, 1731-1741.

Kudanga, T., Nyanhongo, G.S., Guebitz, G.M., Burton, S., 2011. Enzyme Microb. Technol. 48, 195-208.

Lanzellotto, C., Favero, G., Antonelli, M.L., Tortolini, C., Cannistraro, S., Coppari, E., Mazzei, F., 2014. Biosens. Bioelectron. 55, 430-437.

Liu, C.-H., Chang, Y.-C., Norris, T.B., Zhong, Z., 2014. Nat. Nanotechnol. 9, 273-278.

Mak, K.F., Lee, C., Hone, J., Shan, J., Heinz, T.F. 2010. Phys. Rev. Lett. 105, art. no. 136805.

Mao, K., Wu, Z., Chen, Y., Zhou, X., Shen, A., Hu, J., 2015. Talanta 132, 658-663.

Mazloum-Ardakani, M., Aghaei, R., Abdollahi-Alibeik, M., Moaddeli, A., 2015. J. Electroanal. Chem. 738, 113-122.

Mihalache, I., Radoi, A., Mihaila, M., Munteanu, C., Marin, A., Danila, M., Kusko, M., Kusko, C., 2015. Electrochim. Acta 15, 306-315.

Mihalache, I., Radoi, A., Munteanu, C., Kusko, M., Kusko, C., 2014. Org. Electron. 15, 216-225.

Muthurasu, A., Ganesh, V., 2014. Appl. Biochem. Biotechnol. 174, 945-959.

Nazari, M., Kashanian, S., Rafipour, R., 2015. Spectrochim. Acta, Part A 145, 130-138.

Oliveira, T.M.B.F., Fátima Barroso, M., Morais, S., De Lima-Neto, P., Correia, A.N., Oliveira, M.B.P.P., Delerue-Matos, C., 2013. Talanta 106, 137-143.

Pang, S., Hernandez, Y., Feng, X., Müllen, K., 2011. Adv. Mater. 23, 2779-2795.

Radoi, A., Litescu, S.-C., Eremia, S.A.V., Miu, M., Danila, M., Dinescu, A., Radu, G.-L., 2011. Microchim. Acta 175, 97-104.

Rawal, R., Chawla, S., Devender, Pundir, C.S., 2012. Enzyme Microb. Technol. 51, 179-185.

Razmi, H., Mohammad-Rezaei, R., 2013. Biosens. Bioelectron. 41, 498-504.

Schwierz, F., 2010. Nat. Nanotechnol. 5, 487-496.

Shen, J., Zhu, Y., Yang, X., Li, C., 2012. Chem. Commun. 48, 3686-3699.

Shraddha, Shekher, R., Sehgal, S., Kamthania, M., Kumar, A., 2011. Enzyme Res. 2011, art. no 217861.

Song, H., Ni, Y., Kokot, S., 2014. Biosens. Bioelectron. 56, 137-143.

Soon, J.M., Loh, K.P., 2007. Electrochem. Solid-State Lett. 10, 250-254.

Wang, G.-X., Bao, W.-J., Wang, J., Lu, Q.-Q., Xia, X.-H., 2013. Electrochem. Commun. 35, 146-148.

Wang, T., Zhu, H., Zhuo, J., Zhu, Z., Papakonstantinou, P., Lubarsky, G., Lin, J., Li, M., 2013. Anal. Chem. 85, 10289-10295.

Wang, Zhiming M., 2014. Edited by Zhiming M. Wang. Vol. Lecture Notes in Nanoscale Science and Technology 21. Springer.

Wu, Y., Jiang, Y., Jiao, J., Liu, M., Hu, F., Griffiths, B.S., Li, H., 2014. Colloids Surf., B 114, 342-348.

Zhao, J., Chen, G., Zhu, L., Li, G., 2011. Electrochem. Commun. 13, 31-33.

Zhu, C., Zeng, Z., Li, H., Li, F., Fan, C., Zhang, H., 2013. J. Am. Chem. Soc. 135, 5998-6001.

Fig. 1. Schematic representation of components used for CSPE-MoS_2-GQDs-TvL biosensor construction and the detection principle.

Fig. 2. Fluorescence and UV-Vis absorption (inset) spectra of GQDs.

Fig. 3. Cyclic voltammograms of 1 mM $[Fe(CN)_6]^{3-/4-}$ in 0.1 M KCl on CSPE, CSPE-MoS_2, CSPE-GQDs and CSPE-MoS_2-GQDs; scan rate 50 mV s^{-1}.

Fig. 4. Cyclic voltammograms of 2.5 mM caffeic acid in 0.1 M acetate buffer pH 5.0 (with 0.1 M KCl) at CSPE-TvL, CSPE-MoS_2-TvL, CSPE-GQDs-TvL and CSPE-MoS_2-GQDs-TvL; scan rate 50 mV s^{-1}.

Highlights

- Graphene quantum dots (GQDs) were able to supply excellent electronic conductivity.
- MoS_2 nanoflakes and GQDs drastically decreased the charge-transfer resistance.
- The developed probe assessed the total polyphenolic content from red wines.

Table 1. Analytical parameters of the CSPE-MoS_2-GQDs-TvL biosensor in the determination of polyphenolic compounds.

Compound	Linear range (µM)	Sensitivity (nA µM^{-1})	R^2	LoD* (µM)	K_m^{app} (µM)
Caffeic acid	0.38-10.00	17.92 ± 0.21	0.9992	0.32	11.25
	10.00-100.00	7.32 ± 0.14	0.9982	-	-
Chlorogenic acid	0.38-8.26	11.25 ± 0.36	0.9990	0.19	1.09
	8.26-100.00	5.63 ± 0.12	0.9972	-	
(-) Epicatechin	2.86-100.00	16.42 ± 0.09	0.9997	2.04	121.80

* LoD: 3.3 × intercept standard error/sensitivity

Table 2. Comparison of total polyphenolic content obtained for five red wines with the CSPE-MoS_2-GQDs-TvL biosensor by chronoamperometry in 0.1 M acetate buffer pH 5.00 at a fixed potential of 50 mV *vs.* Ag pseudo-reference electrode and total polyphenolic content obtained using Folin-Ciocalteu method.

Wine sample	**CSPE-MoS_2-GQDs-TvL biosensor (mM)**	**Folin-Ciocalteu method (mM)**
Negru Aromat ICDVV 2013	18.93 ± 1.15	17.09 ± 0.07
Feteasca Neagra ICDVV 2014	11.25 ± 0.88	12.52 ± 0.75
Cabernet Sauvignon Beciul Domnesc 2007	15.50 ± 1.93	16.69 ± 0.17
Pinot Noir Beciul Domnesc 2009	10.04 ± 0.96	14.94 ± 0.26
Feteasca Neagra Beciul Domnesc 2009	15.91 ± 0.89	18.79 ± 0.14